

APPLICATION OF CONVOLUTIONAL NEURAL NETWORKS IN WALL MOISTURE IDENTIFICATION BY EIT METHOD

Grzegorz Kłosowski¹, Tomasz Rymarczyk²

¹Lublin University of Technology, Faculty of Management, Lublin, Poland, ²University of Economics and Innovation in Lublin, Institute of Computer Science and Innovative Technologies, Lublin, Poland

Abstract. The article presents the results of research in the area of using deep neural networks to identify moisture inside the walls of buildings using electrical impedance tomography. Two deep neural networks were used to transform the input measurements into images of damp places - convolutional neural networks (CNN) and recurrent long short-term memory networks LSTM. After training both models, a comparative assessment of the results obtained thanks to them was made. The conclusions show that both models are highly utilitarian in the analyzed problem. However, slightly better results were obtained with the LSTM method.

Keywords: machine learning, deep learning, electrical impedance tomography, moisture detection in walls

ZASTOSOWANIE KONWOLUCYJNYCH SIECI NEURONOWYCH W IDENTYFIKACJI ZAWILGOCEŃ ŚCIAN BUDYNKÓW METODĄ EIT

Streszczenie. W artykule przedstawiono rezultaty badań w obszarze wykorzystania głębokich sieci neuronowych do identyfikacji zawilgoceń wewnątrz ścian budynków przy użyciu elektrycznej tomografii impedancyjnej. Do przekształcenia pomiarów wejściowych na obrazy przedstawiające zawilgocone miejsca użyto dwóch rodzajów głębokich sieci neuronowych – konwulucyjne sieci neuronowe (CNN) i rekurencyjne sieci typu LSTM. Po wytrenowaniu obu modeli dokonano oceny porównawczej uzyskanych dzięki nim rezultatów. Wnioski wskazują na dużą użyteczność obu modeli w badanej problematyce, jednak nieco lepsze rezultaty uzyskano dzięki metodzie LSTM.

Słowa kluczowe: uczenie maszynowe, głębokie uczenie, tomografia impedancyjna, wykrywanie wilgoci w ścianach

Introduction

The presence of moisture inside the walls of buildings is the cause of many unfavourable phenomena. One of them is the chemical and physical degradation of walls, which leads to the weakening of the structure of buildings, reducing their strength. Wet walls crack at low temperatures due to freezing. Chemical compounds, especially aggressive salts and chlorides, which penetrate deep into the walls through faulty foundation insulation, accelerate the erosion of porous materials such as bricks, cement and plaster. The phenomenon of capillary leakage contributes to the spread of moisture areas inside the walls. Moisture destroys plasters and paints coats, worsening the aesthetics. It, in turn, necessitates more frequent renovations, which raises the operating costs of buildings [1]. A separate aspect is the negative impact of moisture on the health and comfort of people staying inside damp rooms. Due to favourable conditions, fungi and microorganisms often breed and multiply inside wet walls. Penetrating humans' breathe causes allergies and other respiratory illnesses [2].

This article presents a non-invasive method to identify moisture inside walls using electrical impedance tomography. Particular attention was paid to the issue of converting electrical measurements generated by tomograph electrodes into spatial images (reconstructions) visualizing moisture areas. The transformation of 96 input measurements into 6215 pixels of the output image resolves an inverse problem that is undefined [1]. For this purpose, a convolutional neural network (CNN) and a deep recurrent long short-term memory network (LSTM) with regressive outputs were used [2].

The novelty of the presented solution is the adaptation of the deep neural network structure, which as a rule is designed for image classification problems to solve the regression problem in which the input is not an image but a vector consisting of 96 voltage measurements. Furthermore, the layers' types, amounts, and parameters were finetuned such that the neural network was effective in learning. As a result, reconstruction images were obtained, the quality of which is adequate to identify areas of moisture inside the walls with sufficient precision.

1. Materials and methods

In order to verify the effectiveness of CNN in the problem of identifying moisture inside the walls of buildings using electri-

cal impedance tomography (EIT) [3, 4], a set of simulation cases was generated. The data set included 40,000 measurement vectors (inputs) and pattern images (outputs). Each measurement vector consisted of 96 measurements correlated with the voltages measured between the different electrode pairs. In order to generate the training data, the EIDORS toolbox was used, which cooperates with the Matlab software. EIDORS works based on the finite element method [5]. A set of 16 linearly positioned electrodes was used in the tests. The scheme of the test stand is shown in Fig. 1.



Fig. 1. Scheme of the measuring stand [6]

The forward problem is solved by determining the potential distribution within the region given the boundary conditions and complete information about the region, i.e. by solving Laplace's equation:

$$-\nabla \cdot (\sigma \nabla u) = 0 \quad (1)$$

where σ denotes conductivity, symbol u represents electrical potential. The optimized fitness function is constructed in the following way:

$$F_{fit} = 0.5 \sum_{i=1}^n (\mathbf{U} - \mathbf{U}_m)^T (\mathbf{U} - \mathbf{U}_m) \quad (2)$$

where n is a projection angle (the number of measurement sequences: 12 measurements \times 8 angle projections = 96 independent measurements), \mathbf{U}_m – the measured voltage, \mathbf{U} – the calculated voltage by solving the equation (1). Fig. 2 shows the way of transforming measurements into tomographic images.

On the surface of the damp brick wall, there are 16 electrodes arranged vertically in a straight line. The electrodes were connected to the EIT tomograph, which manages the measurement

process [5, 7]. Built-in multiplexer determines the frequency of measurements and the sequence of changes of electrode pairs between which the measurement is made. The recorded measurements are then converted into images using CNN and LSTM. The resolution of the spatial image mesh is 6215 finite elements (pixels).

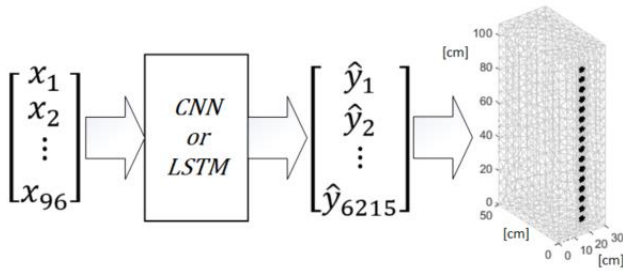


Fig. 2. The method of transforming measurements into tomographic images

In order to better compare the usefulness of deep learning methods in electrical tomography, two types of networks were trained: CNN and LSTM. The structure of the layers of the CNN network is shown in Fig. 3. All used in the CNN fully connected layers model and the regression output layer have the same number of outputs, amounting to 6215.

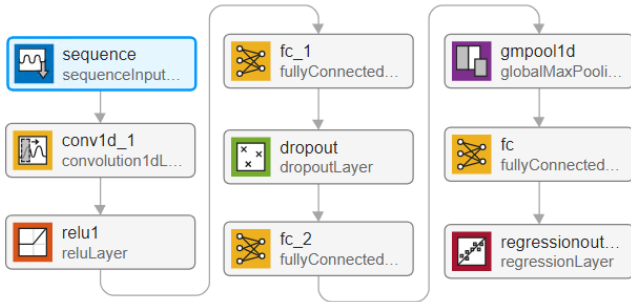


Fig. 3. Convolutional neural network (CNN) layers

The CNN network consists of 9 layers. The first layer has a single sequence structure. It is a vector of 96 measurements. The second layer is a 1-D convolutional layer that applies sliding convolutional filters to 1-D input. It contains 192 filters of size 4. Next is the Rectified Linear Unit (ReLU) layer. The next layer is a fully connected layer that precedes the dropout layer with a probability of 0.3. The sixth layer is connected again, followed by the global max-pooling layer. A fully connected layer multiplies the input by a weight matrix and adds a bias vector. The eighth layer is the third fully connected layer that precedes the regression output layer that computes the half-mean-squared-error loss for regression tasks.

The LSTM model had only 4 layers as shown in Fig. 4. First, the sequence input layer injects sequence data into the network.

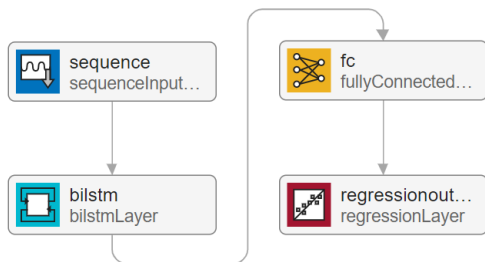


Fig. 4. LSTM network layers

A bidirectional LSTM (BiLSTM) layer learns long-term bidirectional dependencies between time steps of time series or sequence data. These dependencies are advantageous when the network is required to learn from the entire time series at each

time step. The last two layers are the fully connected and regression output layers.

Fig. 5 shows the CNN learning process based on Root Mean Square Error (RMSE). RMSE is calculated according to formula (3)

$$RMSE = \sqrt{\frac{\sum_{i=1}^N (y_i - \hat{y}_i)^2}{N}}, \quad (3)$$

where N is the number of responses, y_i is the target output, and \hat{y}_i is the model's prediction for response i . In addition, Fig. 6 shows the same CNN learning flow but based on the Loss value. The Loss is calculated as (4)

$$Loss = \frac{1}{2S} \sum_{i=1}^S \sum_{j=1}^N (y_{ij} - \hat{y}_{ij})^2, \quad (4)$$

where S is the sequence length. In our case $S = 96$.

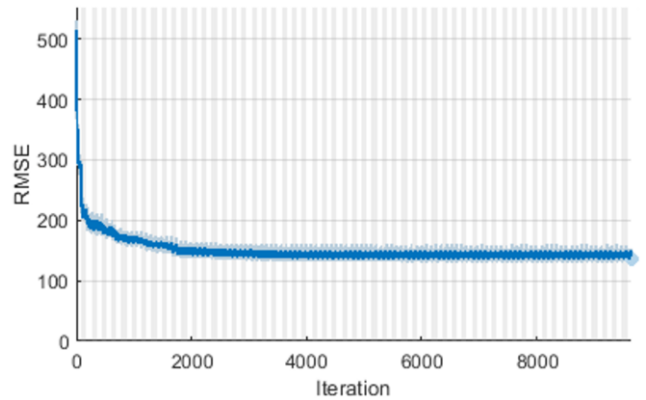


Fig. 5. Training progress of the CNN through the RMSE indicator

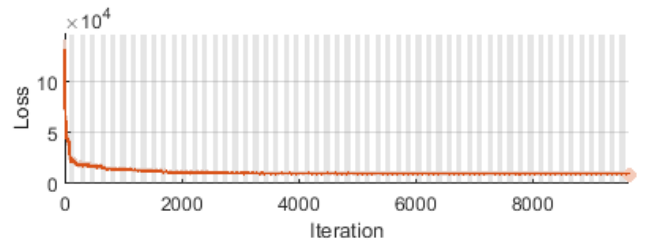


Fig. 6. Training progress of the CNN through the Loss indicator

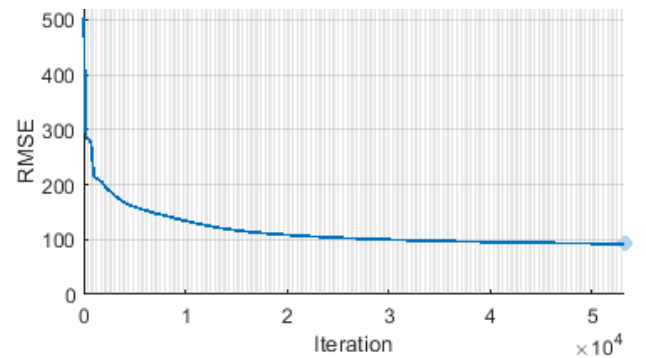


Fig. 7. Training progress of the LSTM through the RMSE indicator

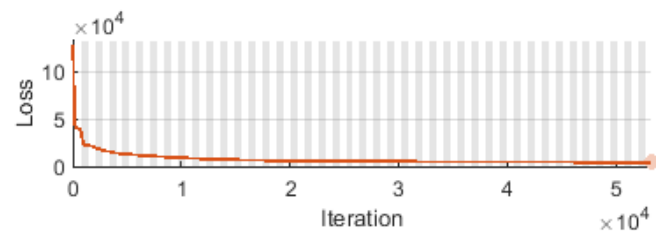


Fig. 8. Training progress of the LSTM through the Loss indicator

As can be seen from the figures above, CNN RMSE is around 145 and Loss around 10^4 . In Figs. 7 and 8 show analogous indicators of the learning quality of the LSTM network. RMSE and Loss here are respectively 95 and $5 \cdot 10^3$. It proves the advantage of

LSTM over CNN. The RMSE and Loss values result from the assumptions made, according to which the background value (dry areas) of the tomographic image is 1, and the moist areas are 10.

2. Results and discussion

Fig. 9 shows the results obtained using CNN and LSTM methods for selected 3 cases. The first case (Fig. 9 a-c) shows

the moisture located in the rear part of the examined area. The LSTM reconstructions seem to be more precise because CNN shows the moisture area larger than in the reference image.

The second case (Fig. 9 d-f) shows the moisture located in the front part of the examined area. Although the LSTM reconstructions seem to be better again, CNN shows areas with different moisture levels also in other parts of the section of the wall, which makes it difficult to identify wet areas correctly.

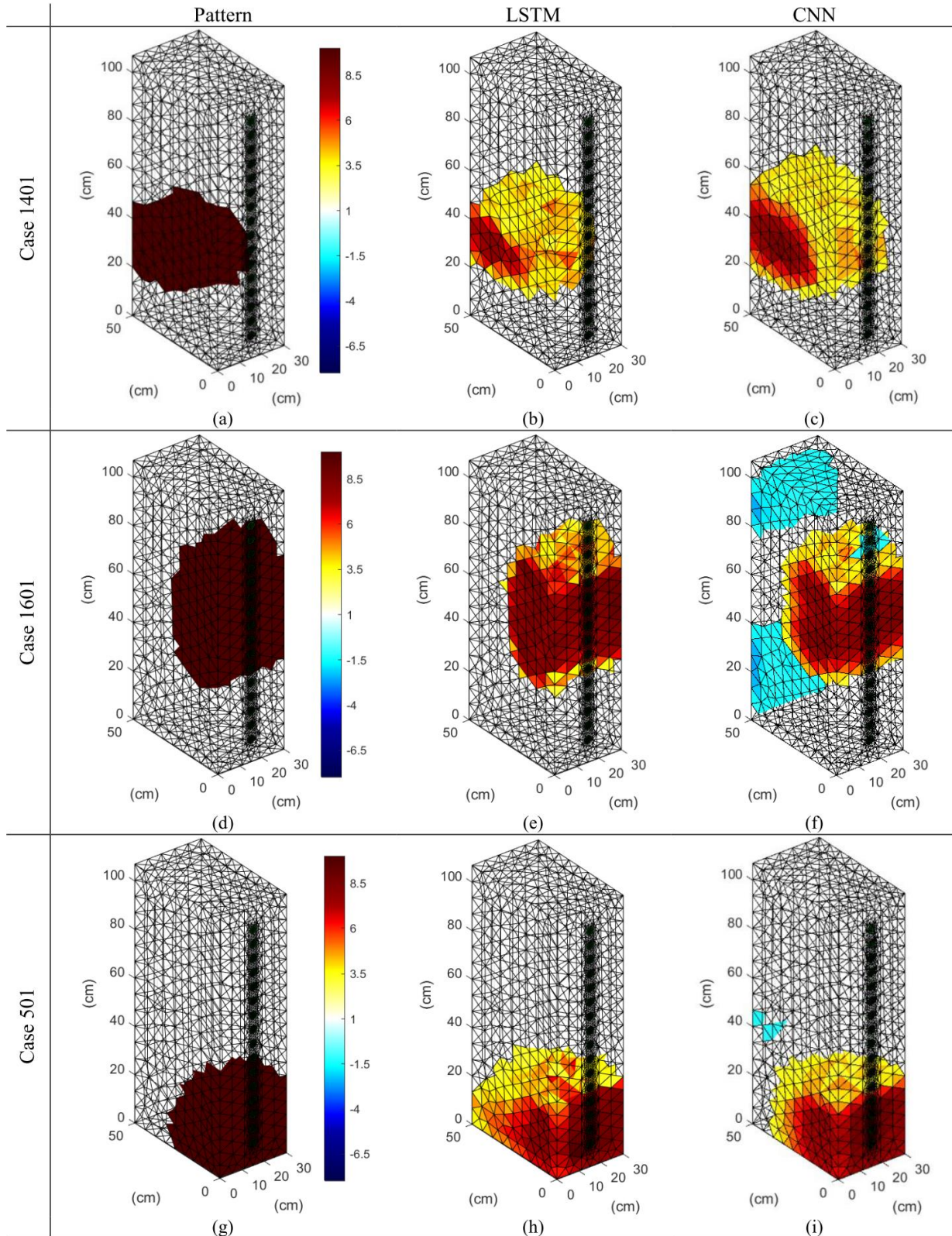


Fig. 9. Comparison of selected reconstructions. Images (a,d,g) are the patterns. Images (b,e,h) were obtained with LSTM algorithm. Images (c,f,i) were created with the CNN algorithm

The third case (Fig. 9 g-i) shows the moisture located in the front lower part of the examined area. Of all the presented cases, this one seems to be the closest for both methods (CNN and LSTM). The shape and contour of the moisture better reflect the CNN, but at the same time, there are minor disturbances in the rear part of the tested section, approximately 40 cm above the ground level.

Four widely used metrics were used to evaluate the quality of tomographic reconstructions objectively: root mean square error (RMSE), normalized mean square error (NMSE), relative image error (RIE), and image correlation coefficient (ICC). The root mean square error is calculated according to the previously presented formula (3). NMSE is calculated by (5)

$$NMSE = \frac{\|y - \hat{y}\|^2}{\|y - \bar{y}\|^2}, \quad (5)$$

where y is the reference (ground-truth) conductivity distribution, \bar{y} is the average reference ground-truth conductivity distribution, \hat{y} denotes the reconstructed conductivity distribution, and $\|\cdot\|$ is the L2-norm set [8,9]. RIE is calculated according to formula (6)

$$RIE = \frac{\|y - \hat{y}\|}{\|y\|}, \quad (6)$$

and ICC is described by equation (7)

$$ICC = \frac{\sum_{i=1}^n (y_i - \bar{y})(\hat{y}_i - \bar{\hat{y}})}{\sqrt{\sum_{i=1}^n (y_i - \bar{y})^2 \sum_{i=1}^n (\hat{y}_i - \bar{\hat{y}})^2}}, \quad (7)$$

where $\bar{\hat{y}}$ is the mean reconstruction conductivity distribution. The lower the RMSE, NMSE, and RIE, and the greater the ICC, the higher the tomographic image quality. ICC = 1 indicates ideal reconstruction, whereas ICC = 0 signifies the worst one.

The Table 1 compares the LSTM and CNN methods. Four criteria defined as indicators were used for this purpose: RMSE, NMSE, RIE, and ICC.

Table 1. Reconstruction quality indicators for the three cases compared

Methods of reconstruction	Indicator	Reconstruction cases		
		Case 1	Case 2	Case 3
CNN	RMSE	1.572	1.781	1.323
	NMSE	0.379	0.244	0.158
	RIE	0.587	0.325	0.275
	ICC	0.722	0.900	0.935
LSTM	RMSE	1.159	1.027	1.261
	NMSE	0.206	0.081	0.143
	RIE	0.433	0.187	0.262
	ICC	0.849	0.968	0.941
Winning method:		LSTM	LSTM	LSTM
		LSTM	LSTM	LSTM
		LSTM	LSTM	LSTM
		LSTM	LSTM	LSTM

Three distinct moisture content cases were evaluated. The table's final four lines contain information about the method that produces the best result for a given case when each measure is considered. As can be seen, the LSTM method produced superior results in all cases evaluated. It should be stated objectively that some of the differences are quite minor. For instance, the difference is very small when comparing the ICC values for Case 3. The delta (difference) ICC is only 0.006. When comparing the two methods, one additional consideration should be made: the reconstruction time. The model's ability to generate images quickly is critical, even more so when performing measurements during dynamic industrial processes. The time required for the LSTM reconstruction was 0.006390 seconds, while the time required for the CNN reconstruction was 0.035113 seconds. In practice, the difference favours the LSTM more than 5 times.

3. Conclusions

This article introduces an innovative algorithmic concept for solving the static problem of tomographic image reconstruction using a recurrent deep LSTM network and convolutional neural network. Electrical impedance tomography was used to image moisture within a brick wall. The LSTM and CNN networks were successfully trained by treating the measurement vector as a single time step sequence signal. The reconstruction's high quality was confirmed by comparing it to images generated using another high-efficiency method, LSTM. Both methods described here allow for spatial visualization of the moisture distribution within a wall. It is significantly different from traditional indirect methods, which only test the humidity at selected wall points. In addition, the LSTM method has a significant advantage in terms of reconstruction speed, which opens up new application possibilities, particularly in the area of automated, dynamic industrial processes. Future research will focus on deciphering the moisture expansion processes occurring within porous materials. To fully exploit the LSTM and CNN networks' potential, more sophisticated modifications to the input vector and data preprocessing are planned.

References

- [1] Fabijańska A., Banasiak R.: Graph Convolutional Networks for Enhanced Resolution 3D Electrical Capacitance Tomography Image Reconstruction. *Applied Soft Computing* 110, 2021, 107608, [http://doi.org/10.1016/j.asoc.2021.107608].
- [2] Hola A.: Measuring of the Moisture Content in Brick Walls of Historical Buildings-the Overview of Methods. *IOP Conference Series: Materials Science and Engineering* 251(1), 2017, [http://doi.org/10.1088/1757-899X/251/1/012067].
- [3] Kłosowski G. et al.: Quality Assessment of the Neural Algorithms on the Example of EIT-UST Hybrid Tomography. *Sensors* 20(11), 2020, [http://doi.org/10.3390/s20113324].
- [4] Kłosowski G. et al.: The Concept of Using Lstm to Detect Moisture in Brick Walls by Means of Electrical Impedance Tomography. *Energies* 14(22), 2021, [http://doi.org/10.3390/en14227617].
- [5] Liti G. et al.: Hygrothermal Performance Evaluation of Traditional Brick Masonry in Historic Buildings. *Energy and Buildings* 105, 2015, 393–411, [http://doi.org/10.1016/j.enbuild.2015.07.049].
- [6] Porzuczek J.: Assessment of the Spatial Distribution of Moisture Content in Granular Material Using Electrical Impedance Tomography. *Sensors* 19(12), 2019, 2807, [http://doi.org/10.3390/s19122807].
- [7] Romanowski A. et al.: X-Ray Imaging Analysis of Silo Flow Parameters Based on Trace Particles Using Targeted Crowdsourcing. *Sensors* 19(15), 2019, 3317, [http://doi.org/10.3390/s19153317].
- [8] Rymarczyk T. et al.: Area Monitoring Using the ERT Method with Multisensor Electrodes. *Przegląd Elektrotechniczny* 95(1), 2019, [http://doi.org/10.15199/48.2019.01.39].
- [9] Rymarczyk T., Adamkiewicz P.: Nondestructive Method to Determine Moisture Area in Historical Building. *Informatics Control Measurement in Economy and Environment Protection* 7(1), 2017, [http://doi.org/10.5604/01.3001.0010.4586].

Ph.D. Eng. Grzegorz Kłosowski
e-mail: g.klosowski@pollub.pl

Assistant Professor in Department of Organization of Enterprise at the Faculty of Management of Lublin University of Technology. The author's research interests include artificial intelligence, simulation, and modelling of engineering and business processes – leader and participant in several implementation projects.

<http://orcid.org/0000-0001-7927-3674>

D.Sc. Tomasz Rymarczyk
e-mail: tomasz.rymarczyk@netrix.com.pl

Director in Research and Development Center Netrix S.A. His research area focuses on applying non-invasive imaging techniques, electrical tomography, image reconstruction, numerical modelling, image processing and analysis, process tomography, software engineering, knowledge engineering, artificial intelligence and computer measurement systems.

<http://orcid.org/0000-0002-3524-9151>

